2. Gough, V. E.; Parkinson, D. *Trans. Inst. Rubber Ind.* **1941**, *17*, 168.
3. Mead, J.; Singh, S.; Roylance, D.; Patt, J. *Polymer Eng. Sci.* **1987**, *27*, 131.
4. Denecour, R. L.; Gent, A. N. J. *Polym. Sci., Part A-2* **1968**, *6*, 1853.
5. Engelhardt, M. L. In *Proceedings of the Rubber Division 150th Meeting*; American Chemical Society: Louisville, Kentucky, 1996.
6. Gent, A. N.; Hindi, M. *Rubber Chem. Technol.* **1988**, *61*, 892.
7. Campbell, D. S. *J. Appl. Polym. Sci.* **1970**, *14*, 1409.
8. Morrison, N. J.; Porter, M. *Rubber Chem. Technol.* **1984**, *57*, 63.
9. Cunneen, J. I.; Russell, R. M. *Rubber Chem. Technol.* **1970**, *43*, 1215.
10. Choi, S.-S. *Korea Polym. J.* **1997**, *5*, 39.
11. Krejsa, M. R.; Koenig, J. L. *Rubber Chem. Technol.* **1993**, *66*, 376.
12. Rostek, C. J.; Lin, H.-J.; Sikora, D. J. In *Proceedings of the Rubber Division 143rd Meeting*; American Chemical Society: Denver, Colorado, 1993.
13. Hands, D.; Horsfail, F. *Rubber Chem. Technol.* **1977**, *50*, 253.
14. Sircar, A. K.; Wells, J. L. *Rubber Chem. Technol.* **1982**, *55*, 191.

Dynamics of Poly[oxy-1,4-phenyleneoxy-2-{6-(4-(4-butylphenylazo) phenoxy)hexyloxy}terephthaloyl] and Poly[oxy-1,4-phenyleneoxy-2-{10-(4-(4-butylphenylazo)phenoxy)decyloxy}terephthaloyl] Studied by ^{13}C CP-MAS NMR

Gyunggoo Cho[‡], Oc Hee Han*, and Jung-Il Jin[†]

Korea Basic Science Institute, Taejon 305-333, Korea
[†]Department of Chemistry and Advanced Materials Chemistry Research Center, Korea University, Seoul 136-701, Korea
Received August 25, 1997

Carbon-13 CP-MAS NMR techniques were used to investigate dynamics of new combined type liquid crystalline polymers, poly[oxy-1,4-phenyleneoxy-2-{6-(4-(4-butylphenylazo)phenoxy)hexyloxy}terephthaloyl] and poly[oxy-1,4-phenyleneoxy-2-{10-(4-(4-butylphenylazo)phenoxy)decyloxy}terephthaloyl]. Noticeable mobility change of either aromatic groups or methylene groups is not detected between 25 ℃ and 82 ℃ from ^{13}C spin-lattice relaxation time in the rotating frame ($T_{1\rho}(C)$) and contact time array experiments. However, line shape analysis shows the increase of mobility of methylene carbons in poly[oxy-1,4-phenyleneoxy-2-{6-(4-(4-butylphenylazo)phenoxy)hexyloxy}terephthaloyl] at higher temperature. The dynamics of side chains does not seem to be affected in our experimental temperature range by the length of aliphatic chain which is connecting the side chain group to the main chain.

Introduction

The macroscopic physical properties of solid polymers are mainly determined by their molecular level structure and dynamics. Orientational order plays an important role in solid polymers. The degree of orientation is enhanced by drawing, which leads to the improvement of mechanical properties. Molecular dynamics also influences physical properties, for example, the molecular motion of the rates in the range of the frequency of the alternating mechanical or electric fields is strongly correlated with a change of dynamic moduli or compliances.[1-3] The energy-dissipating local molecular motion slowed down too much produces brittle materials, on the other hand, the increase of molecular motion can result in the decrease of the strength of the materials.[1]

New combined type liquid crystalline polymers(LCP), poly[oxy-1,4-phenyleneoxy-2-{6-(4-(4-butylphenylazo) phenoxy)hexyloxy}terephthaloyl] and poly[oxy-1,4-phenyleneoxy-2-{10-(4-(4-butylphenylazo)phenoxy)decyloxy}terephthaloyl] (from now on, will be abbreviated as PAZO-6 and PAZO-10, respectively), consist of poly(*p*-terephthalate) main chain and azo group with a aliphatic chain, as a side chain, attached to the main chain. The molecular formulas of the PAZO samples are shown in Scheme 1, where n indicates the number of methylene carbon between poly(*p*-terephthalate) and the azo group (n is 6 in PAZO-6 and 10 in PAZO-10). Since the alkyl chain length of the side chains may influence the structure and dynamics of the polymers, it is worthwhile to compare the structure and dynamics of PAZO-6 and PAZO-10.

NMR line shapes are sensitive to molecular motions. As the motions are fast and isotropic, the line shapes become narrow in the extreme narrowing limit. In general, the observed full line width at half height $(\pi T_2)^{-1}$ can be described as

[‡]Present address: Kumho Tire Co. R & D Center 555 Sochon-dong Kwangsan-gu Kwangju Korea 506-040

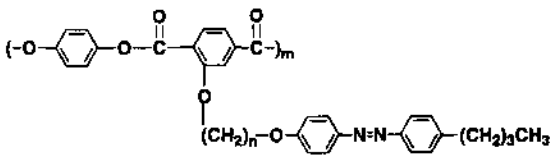

Scheme 1.

$$1/\pi T_2 = 1/\pi T_{2m} + 1/\pi T_{2\sigma} + 1/\pi T_{2res}$$

where $1/\pi T_{2m}$ is motional line broadening due to heteronuclear dipole coupling modulation, $1/\pi T_{2\sigma}$ is motional line broadening due to motional modulation of ^{13}C chemical shift anisotropy (chemical shift distribution due to a molecule's orientational difference in the external magnetic field), $1/\pi T_{2res}$ is static line broadening due to bulk susceptibility of the samples and isotropic chemical shift dispersions from packing effects, bond distortions, and conformational differences.[4,5] Here, the full width at half heights are expressed in the notation of spin-spin relaxation times. For protonated carbons, motional line broadening due to heteronuclear dipole coupling modulation is typically the main cause of line broadening. T_{2m} is equal to ^{13}C spin-lattice relaxation time in the rotating frame ($T_{1\rho}(C)$) under a certain condition.[4,5] The condition includes Hartmann-Hahn matching, exact on-resonance proton irradiation, and negligible adiabetic magnetization transfer to proton. $T_{2\sigma}$ attributes recognizable line broadening for carbons with large chemical shift anisotropy such as aromatic and carbonyl carbons.[4,5]

Local motions of polymers can be probed using $T_{1\rho}(C)$ since ^{13}C spin diffusion[6,7] and the adiabetic magnetization transfer to proton are negligible in glassy polymers like our samples.[5] $T_{1\rho}(C)$ is most sensitive to the motion in the frequency of carbon RF field, typically several tens of kHz.

Carbon-13 cross polarization-magic angle spinning (CP-MAS) NMR also can give information about molecular structures and dynamics of polymers. Initial nonexponential fast CP transient phenomenon is typically observed from methylene and methine carbons when carbon-proton dipole interaction is stronger than proton-proton dipole interaction.[5] This phenomenon is barely observed and CP transient becomes exponential if large amplitude molecular motion faster than 10^5 kHz causing reduction of dipole interaction exists.[5] On the other hand, CP transients for non-protonated carbons are typically exponential.[8] Even when a rise of carbon intensity by CP is exponential, CP rate is a function of molecular motions.[8] In this work, the structures and dynamics of PAZO-6 and PAZO-10 samples have been investigated by observation of $T_{1\rho}(C)$, CP rates, and line shape change with ^{13}C CP-MAS NMR techniques at various temperatures.

Experimental

The PAZO samples were prepared as described in the previous report.[9] The phase transition temperatures of the samples are summarized in Table 1. All ^{13}C CP-MAS NMR spectra were acquired with a Larmor frequency of 75.46 MHz on a Varian UNITYplus 300 spectrometer at various temperatures between 25 ℃ and 82 ℃. The highest temperature we could safely operate the probe at was 82 ℃.

Table 1. The phase transition temperatures of PAZO samples measured by the differential scanning calorimetry[9]

Samples	T_g	T_m	T_i
PAZO-6	-58 ℃	188 ℃	265 ℃
PAZO-10	-	164 ℃	>300 ℃

*T_g, T_m, and T_i represent glass transition, melting, and isotropic transition temperatures, respectively.

The $\pi/2$ pulse length, contact time, and pulse sequence repetition time were 5.0 μs, 1 ms, and 5 s, respectively. The spinning speed for all spectra was 5.0 kHz to avoid the overlap between centerbands and sidebands. $T_{1\rho}(C)$ was measured using a pulse sequence which involves an array of variable spin locking times after a contact time. The spin lock field of 33.3 kHz as well as 50 kHz were employed. For the comparison of CP rates, intensities of individual peaks versus an array of variable contact times were observed. Dipolar dephasing experiments[10] with dipolar dephasing time of 100 μs was carried out to distinguish protonated and non-protonated carbons. Experimental temperatures were calibrated with ethylene glycol chemical shift.[11]

Result and Discussion

PAZO-6 Figure 1 shows a representative ^{13}C CP-MAS NMR spectrum of PAZO-6 at room temperature and the peak assignments. The assignments of alkyl, alkoxy, aromatic and carbonyl peaks are straightforward. The peak at 14 ppm is assigned to the methyl carbon. The peaks between 20 ppm and 40 ppm belong to methylene carbons.

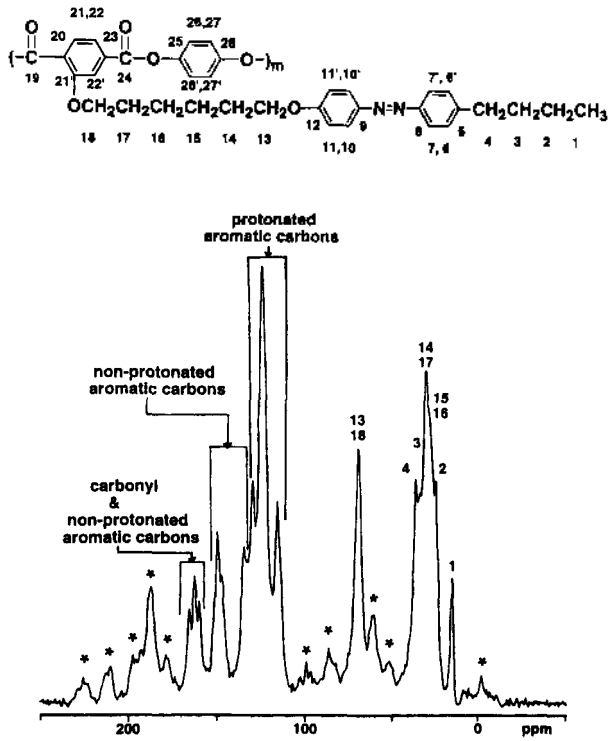

Figure 1. A representative ^{13}C CP-MAS NMR spectrum of PAZO-6 at room temperature with peak assignments. *indicates the spinning sidebands.

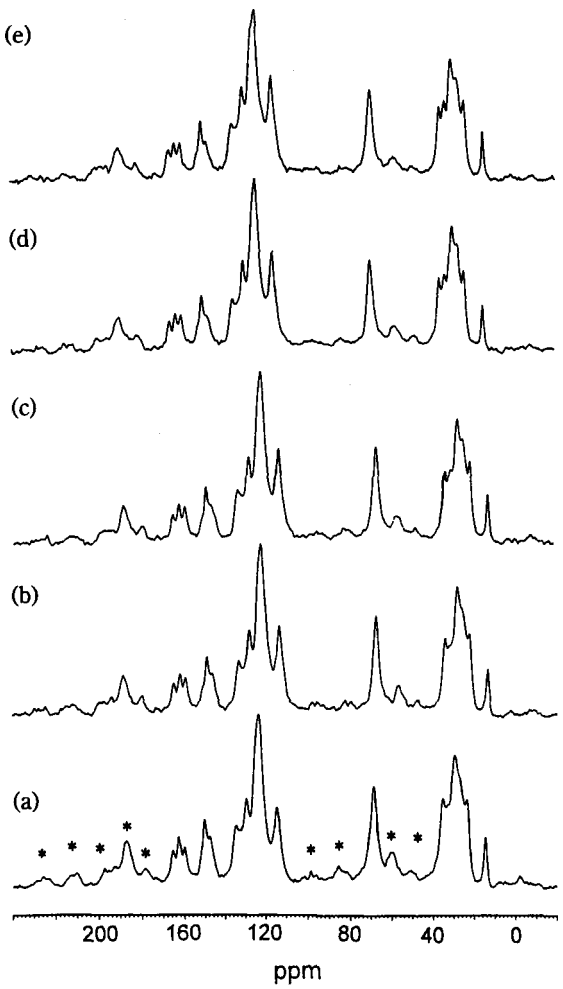

Figure 2. ^{13}C CP-MAS NMR spectra of PAZO-6 at (a) 25 ℃, (b) 38 ℃, (c) 55 ℃, (d) 68 ℃, and (e) 82 ℃. *indicates the spinning sidebands.

Alkoxy carbons resonate at 68 ppm. Most aromatic carbons appear between 110 ppm and 152 ppm. Non-protonated and protonated aromatic carbons have been differentiated using dipolar dephasing experiments. The peaks of protonated carbons decay faster than those of non-protonated carbons as a dipolar dephasing time increases. Most of the signals at 115 ppm, 123 ppm and 129 ppm dephased at dipolar dephasing time of 100 μs. Thus, they can be assigned to the protonated aromatic carbons while the peaks at 134 ppm, 146 ppm and 149 ppm are assigned to non-protonated aromatic carbons. The triplet signal near 162 ppm, which dephased very slowly at the dipolar dephasing experiment, could be from some of non-protonated aromatic carbons as well as carbonyl carbons.

The observation of the line widths of peaks versus temperature can provide information on molecular motion in the polymers. As temperatures increase, the line widths of the methylene peaks decrease while those of the aromatic peaks do not change as shown in Figure 2. Line widths of the methylene peaks obtained from line shape simulation were summarized in Table 2. The narrower line widths of the methylene peaks at higher temperature, resulting in better resolved peaks, indicate the increase of mobility of alkyl chains. But alkoxy carbons do not show any definite line

Table 2. The full width at half height of the methylene peaks obtained from the line shape simulation at each temperature

Temp. (℃)	Full width at half height (Hz)				
	24 ppm	28 ppm	31 ppm	35 ppm	37 ppm
25	1.3×10^2	2.2×10^2	2.4×10^2	2.0×10^2	1.6×10^2
38	1.3×10^2	2.0×10^2	2.1×10^2	1.8×10^2	1.5×10^2
55	1.0×10^2	1.8×10^2	1.9×10^2	1.2×10^2	1.5×10^2
68	0.9×10^2	1.7×10^2	1.8×10^2	1.0×10^2	1.2×10^2
82	0.7×10^2	1.6×10^2	1.7×10^2	1.0×10^2	1.2×10^2

width change. Aromatic peaks from the main chains and the side chains are overlapped. If the line width of aromatic peaks either from the main chains or the side chains changes due to the motional difference at various temperatures, the line shape of aromatic peaks should vary. However, the line shape change of aromatic peaks is not observed in Figure 2. Therefore, line width variation due to dynamics of aromatic or alkoxy carbons is negligible compared to that of methylene carbons in the temperature range of 25 ℃ and 82 ℃.

It is possible that only the three methylene carbons of butyl group in Scheme 1 contribute to the line width change of methylene peaks between 20 and 40 ppm while four methylene carbons between two alkoxy carbons do not at all. However, liquid state NMR results (not shown) of the monomer (solvent: $CDCl_3$) at room temperature indicate that the methylene carbons in the butyl group should contribute to two leftside peaks and one rightside peak among five methylene peaks in the spectrum at high temperatures. Molecular formula of the monomer is described in Scheme 2. Thus, the line width change observed is due to dynamics change of not only the methylene carbons in the butyl group but also the methylene carbons between two alkoxy carbons.

The efficiency of CP is proportional to the effective strength of C-H dipolar interaction which is a function of molecular motion.[8] The increase of motion is expected to result in the longer contact time to reach the maximum ^{13}C intensity due to the lowered efficiency of the CP.[4,5,8] Figure 3 shows the intensities of methylene and aromatic peaks as a function of contact time at various temperatures. The intensity at 30 ppm was taken as a representative methylene peak for the plot since all methylene peaks have the same CP rate and the peak at 30 ppm has the biggest intensity among them. Likewise the peak at 123 ppm was taken as a representative aromatic peak. Initial non-exponential fast CP phenomenon[4,5] typically observed from methylene and methine carbons when carbon-proton dipole interaction is stronger than proton-proton dipole interaction was not clearly detected in PAZO samples. The result suggests that proton-proton dipole interaction is stronger than carbon-proton

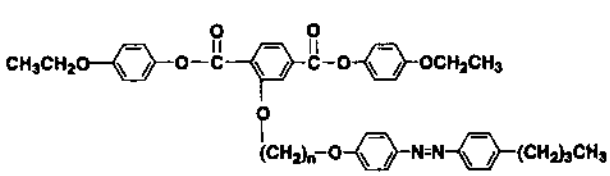

Scheme 2.

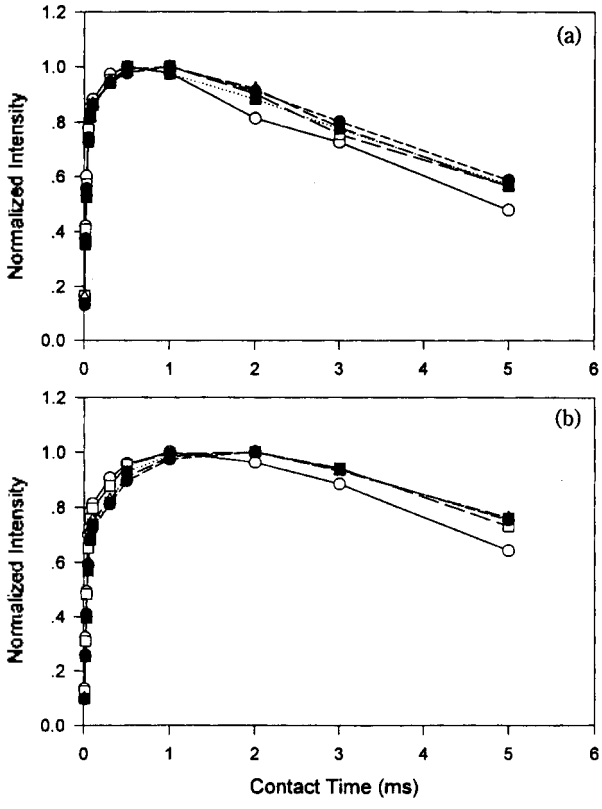

Figure 3. Intensity plots of (a) methylene peak at 30 ppm and (b) aromatic signal at 123 ppm as a function of contact time at 25 ℃ (open circle), 38 ℃ (open square), 55 ℃ (open triangle), 68 ℃ (black circle), and 82 ℃ (black square). All intensities were normalized to the highest peaks at a given temperature.

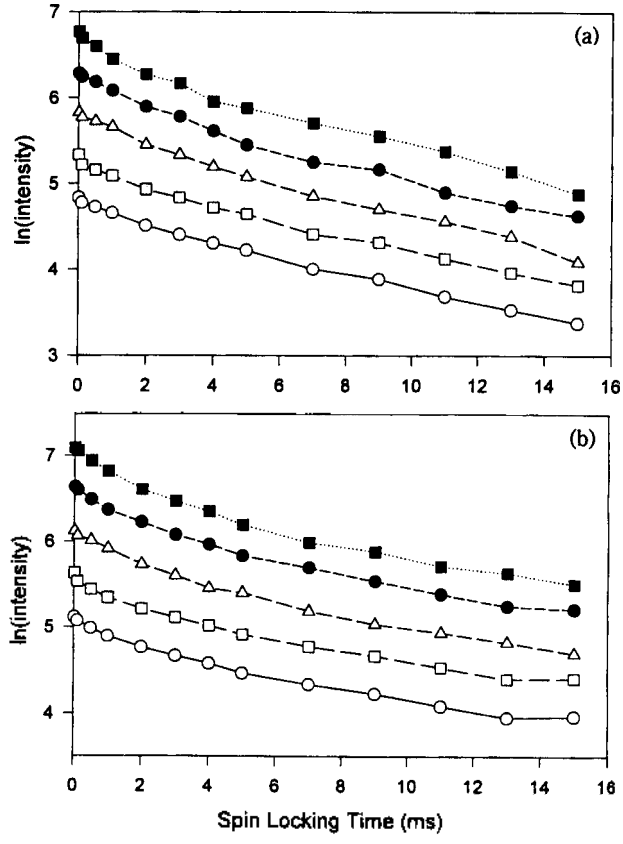

Figure 4. ln(intensity) plots of (a) methylene peak at 30 ppm and (b) aromatic signal at 123 ppm as a function of spin lock time at 25 ℃ (open circle), 38 ℃ (open square), 55 ℃ (open triangle), 68 ℃ (black circle), and 82 ℃ (black square). Different values of intercept was added to see slopes clearly.

dipole interaction in the samples probably due to molecular motion weakening this interaction. The reduced efficiency of the CP was not observed at higher temperature within an experimental error. Thus, molecular dynamics affecting the CP rates, which is faster than 10^5 Hz,[5] must not vary much between 25 ℃ and 82 ℃.

Figure 4 shows the plots of ln(intensity) versus ^{13}C spin lock time of methylene (30 ppm) and aromatic (123 ppm) peaks at various temperatures. The relationship between ln (intensity) and spin lock time deviates from linearity. If intensities decay single-exponentially during the spin lock times, the ln(intensity) versus spin lock times should be linear. However, $T_{1\rho}$(C) can be rarely fitted by a single exponential due to a distribution of correlation times for motion at one site and a number of non-consenting dynamic environments for chemically or structurally equivalent carbons.[6]

The higher temperature (or more motion) could result in the change of the relaxation rate. If the motion is on the low temperature side of the minimum, $T_{1\rho}$(C) decreases as the temperature increases and vice versa. Thus, the spectral density in the mid-kHz can be estimated by the measurement of $T_{1\rho}$(C) as a function of temperature. In Figure 3, intensities are contributed by fast and slow relaxing components not clearly separated at boundaries so that the $T_{1\rho}$(C)s of individual components depend on the number of data points one chooses. Thus, all data points as a whole are compared in the Figure 3 rather than fitting with a couple of relaxation rates for a data set at each temperature. The comparison shows no difference of the relaxation rates at different temperatures. Thus, no difference of $T_{1\rho}$(C)s of the individual components was observed within an experimental error. When the motion is near the minimum (*i.e.*, $\omega\tau_c$~1) the variation of $T_{1\rho}$(C)s could be less sensitive to temperature changes than that on either the high temperature side or the low temperature side. In order to elucidate whether the mobility change of PAZO-6 is small or the motion is near the minimum at the temperature range used, we reduced a spin lock field strength from 50 KHz to 33.3 KHz. The $T_{1\rho}$(C) of the methylene peak at 30 ppm was obtained with the assumption of a single-exponential decay, which declines from 10.5 ms to 3.1 ms for the reduction of the spin lock field strength. The experiment with different spin lock field strengths indicates that the motion of the PAZO-6 sample is on the low temperature side and that molecular motion change of PAZO-6 is not significant in mid kHz range at the temperatures between 25 ℃ and 82 ℃.

In the temperature range of 25 ℃ and 82 ℃, only line widths of methylene carbons were observed to be altered. The changes of CP rates and $T_{1\rho}$(C) were negligible. These results imply that only the motions affecting the line widths of methylene peaks vary substantially in the temperature range. This motional line width averaging could be related with modulation of residual proton-carbon dipolar interaction (T_{2m}) or modulation of chemical shift anisotropy

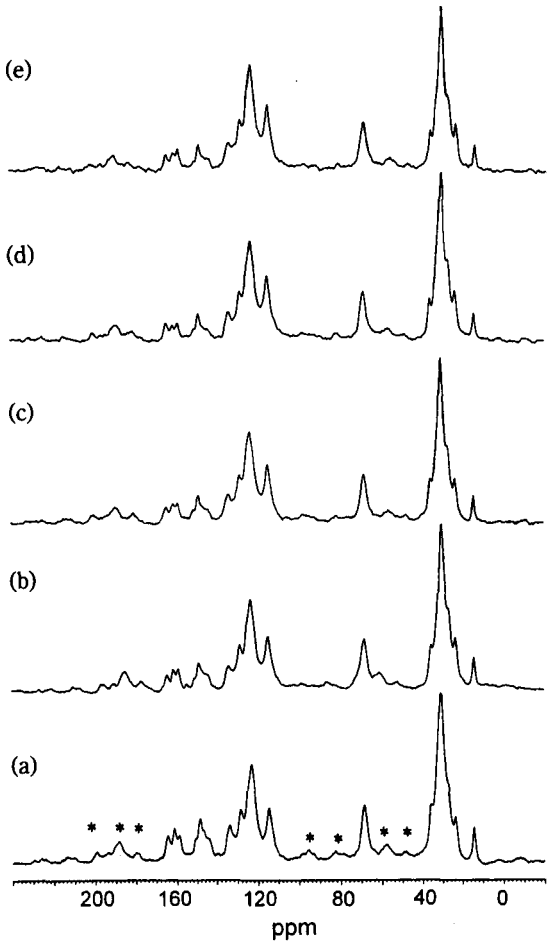

Figure 5. ^{13}C CP-MAS NMR spectra of PAZO-10 at (a) 25 ℃, (b) 38 ℃, (c) 55 ℃, (d) 68 ℃, and (e) 82 ℃. * indicates the spinning sidebands.

($T_{2\sigma}$) or reduction of isotropic chemical shift dispersion (T_{2res}). Our experimental condition satisfies the requirement for the relationship of $T_{1\rho}(C)=T_{2m}$ so that T_{2m} should be almost constant in our experimental temperature range. Chemical shift anisotropy of methylene carbons are inherently small.[5] Then, the line width reduction must be due to averaging of isotropic chemical shift dispersion *via* exchanging phenomena rather than from averaging out residual proton-carbon dipolar interaction.

The chemical shift is influenced by molecular packing, bond distortions, and conformational differences in the solid state resulting in chemical shift dispersion, although this effect seems to result in a dispersion of a few ppm at most. A steric-hindrance model, developed by Grant and Cheney, can be used to predict the ^{13}C chemical shifts of CH perturbed by the additional H atoms nearby in the solid state.[12] The exchanging of the isotropic chemical shifts is expected to occur at low frequencies since the isotropic chemical shift differences of the methylenes in our samples are smaller than a couple of hundred Hz. In MAS spectra, chemical shift anisotropy is already averaged out by MAS.

PAZO-10. Figure 5 shows ^{13}C CP-MAS NMR spectra of PAZO-10 at different temperatures. Line shapes of PAZO-10 spectra are similar to those of PAZO-6, except methylene peaks. All methylene carbons of the alkyl chain connecting azo group to the main chain except alkoxy carbons resonate between 26 and 32 ppm regardless of the chain length. As a result, the longer alkyl chain length leads to severer overlap of methylene peaks so that the resolution of methylene peaks in the PAZO-10 spectrum is lower than that of the PAZO-6 spectrum. This poor resolution made it difficult to detect any methylene line shape change at various temperatures for PAZO-10. Line width change less than a couple of hundred Hz of the peaks in 26-32 ppm would not make the total line shape of methylene resonance region. Thus, methylene carbons of PAZO-10 are expected to have similar exchange phenomena observed in PAZO-6 resulting in the reduction of isotropic chemical shift dispersion but the corresponding line shape change was not observed due to severer overlap of the methylene peaks than those of PAZO-6. Alternatively, methylene carbons of PAZO-10 have smaller or no reduction of isotropic chemical shift dispersion although motion of the side chain of PAZO-10 may be expected to be faster than that of PAZO-6 by means of longer side chain length. The cross polarization efficiency and $T_{1\rho}(C)$ of PAZO-10 also did not differ when temperature increases as of PAZO-6.

Conclusion

High resolution solid state NMR techniques were employed to obtain information on dynamics of PAZO samples with different lengths of alkyl chains which connect azo groups to main chains. There was no definite dynamics difference observed between PAZO-6 and PAZO-10 even though they have different lengths of alkyl chains in the temperature range 25-82 ℃. Motional change of aromatic carbons in main chains or side chains was not observed but methylene carbons in side chains seem to be slightly more mobile at higher temperature.

Acknowledgement. This work was supported in part by the National R & D Project (UCPN00018) administered by the Ministry of Science and Technology in Korea. We would like to thank Ms. Seen Ae Chae at the KBSI and Mr. Jong-Sung Kim at Kumho Chemicals Inc. for NMR technical support and sample preparation, respectively. Mr. Kim synthesized the samples when he was a graduate student at Korea University.

References

1. McCrum, N. G.; Read, B. E.; Williams, G. *Anelastic and Dielectric Effects in Polymeric Solids*; John Wiley & Sons: New York, 1967.
2. Aharoni, S. M.; Sibilia, J. B. *Polymer Engineering and Science* **1979**, *19*, 450.
3. Ward, I. M. *Atlas of Polymer Morphology*; Hanser Verlag: Muchen, 1989.
4. VanderHart, D. L.; Earl, W. L.; Garroway, A. N. *J. Magn. Reson.* **1981**, *44*, 361.
5. Laupretre, F. *High Resolution ^{13}C NMR Investigations of Local Dynamics in Bulk Polymers at Temperatures Below and Above the Glass Transition Temperature In NMR 30*; Solid-State NMR I: Methods, Diehl, P.; Fluck, E.; Gunther, H.; Kosfeld, R.; Seelig, J., Eds.; Springer-Verlag: Berlin, New York, 1994.

6. Schaefer, J.; Stejskal, E. O.; Buchdahl, R. *Macromolecules* **1977**, *10*, 384.
7. Schaefer, J.; Sefcik, M. D.; Stejskal, E. O.; McKay, R. A.; Dixon, W. T.; Cais, R. E. *Macromolecules* **1984**, *17*, 1107.
8. Stejskal, E. O.; Memory, J. D. *High Resolution NMR in the Solid State, Fundamentals of CP/MAS*; Oxford University Press: Oxford and New York, 1994 and references therein.
9. Kim, J.-S. MS thesis, Korea University: Seoul, Korea, 1995.
10. Opella, S. J.; Frey, M. H. *J. Am. Chem. Soc.* **1979**, *101*, 5854.
11. Varian Associates Inc. Nuclear Magnetic Resonance Instruments, Variable Temperature Systems Installation and Maintenance, Publication Number, 87-195402-00, Rev. C0592; Varian Associates Inc.: Palo Aalto, 1989. p 41.
12. Grant, D. M.; Cheney, B. V. *J. Am. Chem. Soc.* **1967**, *89*, 5315.

Polypyrrole Doped with Sulfonate Derivatives of Metalloporphyrin: Use in Cathodic Reduction of Oxygen in Acidic and Basic Solutions

Eui-hwan Song[†] and Woon-kie Paik*

Department of Chemistry, Sogang University, Seoul 121-742, Korea
Received August 25, 1997

Incorporation of metalloporphyrins into polypyrrole (PPy) film was achieved either by electropolymerization of pyrrole in the presence of metal-tetra(sulfonatophenyl)porphyrin anion (MTSPP, M=Co, Fe) or by metalizing hydrogenated tetra(4-sulfonatophenyl)porphyrin anion (H_2TSPP) doped into PPy through ion-exchange. Electrochemical reduction of oxygen on the PPy doped with metallo porphyrin (PPy-MTSPP) was studied in acidic and basic solutions. Oxygen reduction on PPy-MTSPP electrodes appeared to proceed through a 4-electron pathway as well as a 2-electron path. In acidic solutions, the overpotential for O_2 reduction on PPy-CoTSPP electrode was smaller than that on gold by about 0.2 V. In basic solutions the overpotential of the PPy-CoTSPP electrode in the activation range was close to those of Au and Pt. The limiting current was close to that of Au. However, polypyrrole doped with cobalt-tetra(sulfonatophenyl)porphyrin anion (PPy-CoTSPP) or with iron-tetra (sulfonato phenyl) porphyrin anion (PPy-FeTSPP) was found to have limited potential windows at high temperatures (above 50 °C), and hence the electrode could not be held at the oxygen reduction potentials in basic solutions (pH 13) without degradation of the polymer.

Introduction

The search for efficient and cost-effective electrocatalysts for cathodic oxygen reduction other than platinum and its alloys has been intensive because of their importance in applications such as fuel cells and metal/air batteries.[1-3] Metal porphyrins and metal phthalocyanines are among the best candidates because they have excellent thermal and chemical stabilities,[4] and they exhibit excellent catalytic properties.[1,5,6] Incorporating porphyrins into a conducting polymer is one efficient technique for making electrodes with immobilized metalloporphyrins. Incorporation of metalloporphyrin into conducting polypyrrole (PPy) can be achieved by one of three different methods: i) polymerization of pyrrole in the presence of a metalloporphyrin that is derivatized with an anionic group so that the porphyrin anion is incorporated into the polymer matrix as counter-ions for the positively charged polymer;[7-10] ii) Polymerization of porphyrin-substituted pyrrole;[11,12] iii) Ion exchange into polymer of *N*-alkylammonium pyrrole salt.[13,14]

We adopted the first method, *i.e.* incorporation of metalloporphyrins with attached anionic groups into PPy by polymerizing the monomer pyrrole in the presence of the functionalized porphyrins. Cathodic reduction of oxygen on the resulting polymer electrode was studied in acidic and basic aqueous electrolytes using a rotating ring-disk assembly.

Experimental

Deposition of polypyrrole doped with metalloporphyrin. Polypyrrole films doped with metalloporphyrins were prepared by anodic electropolymerization on platinum, gold, or glassy carbon (GC) disk electrodes in aqueous solutions containing 0.1 M pyrrole and 1 mM of the appropriate salt of anionic metalloporphyrin. The anionic metalloporphyrins have a structure shown by the following example of a sulfonated Co-porphyrin.

Sodium salts of cobalt-tetra(sulfonatophenyl)porphyrin anion (CoTSPP), iron-tetra(sulfonato phenyl)porphyrin anion (FeTSPP), and tetra(sulfonatophenyl)porphyrin anion

[†]Present Address: Division of Chemistry and Chemical Engineering, California Institute of Technology, Pasadena, California 91125, U.S.A.